Neurobiology of Aging 36 (2015) 33–41

Contents lists available at ScienceDirect

Neurobiology of Aging

journal homepage: www.elsevier.com/locate/neuaging

Altered cerebrovascular reactivity velocity in mild cognitive impairment and Alzheimer's disease

Jonas Richiardi [a,b,c], Andreas U. Monsch [d], Tanja Haas [e], Frederik Barkhof [f], Dimitri Van de Ville [g,h], Ernst W. Radü [i], Reto W. Kressig [j], Sven Haller [k,*]

[a] Department of Neurology and Neurological Sciences, Stanford University, Stanford, CA, USA
[b] Department of Neurosciences, University of Geneva, Geneva, Switzerland
[c] Department of Neurology, University of Geneva, Geneva, Switzerland
[d] Memory Clinic, University Center for Medicine of Aging Basel, Felix Platter Hospital, Basel, Switzerland
[e] Department of Radiology, University Hospital Basel, Basel, Switzerland
[f] Department of Radiology and Nuclear Medicine, Neuroscience Campus Amsterdam, VU University Medical Centre, Amsterdam, the Netherlands
[g] Department of Radiology and Medical Informatics, Faculty of Medicine, University of Geneva, Genève, Switzerland
[h] Institute of Bioengineering, School of Engineering, EPFL, Lausanne, Switzerland
[i] Medical Image Analysis Center MIAC, University Hospital Basel, Basel, Switzerland
[j] University Center for Medicine of Aging Basel, Felix Platter Hospital, Basel, Switzerland
[k] Service neuro-diagnostique et neuro-interventionnel DISIM, Hôpitaux Universitaires de Genève, Genève, Switzerland

ARTICLE INFO

Article history:
Received 6 March 2014
Received in revised form 15 July 2014
Accepted 18 July 2014
Available online 24 July 2014

Keywords:
Mild cognitive impairment
Alzheimer
Cognitive decline
MRI
Perfusion
Carbon dioxide
Vasoreactivity

ABSTRACT

Interindividual variation in neurovascular reserve and its relationship with cognitive performance is not well understood in imaging in neurodegeneration. We assessed the neurovascular reserve in amnestic mild cognitive impairment (aMCI) and Alzheimer's dementia (AD). Twenty-eight healthy controls (HC), 15 aMCI, and 20 AD patients underwent blood oxygen level–dependent imaging for 9 minutes, breathing alternatively air and 7% carbon dioxide mixture. The data were parcellated into 88 anatomic regions, and carbon dioxide regressors accounting for different washin and washout velocities were fitted to regional average blood oxygen level–dependent signals. Velocity of cerebrovascular reactivity (CVR) was analyzed and correlated with cognitive scores. aMCI and AD patients had significantly slower response than HC (mean time to reach 90% of peak: HC 33 seconds, aMCI and AD 59 seconds). CVR velocity correlated with Mini Mental State Examination in 35 of 88 brain regions ($p = 0.019$, corrected for multiple comparisons), including 10 regions of the default-mode network, an effect modulated by age. This easily applicable protocol yielded a practical assessment of CVR in cognitive decline.

1. Introduction

Vascular alterations are present in several dementias, including Alzheimer's disease (AD) and can appear at an early stage (Claassen et al., 2009). Through neurovascular coupling, vascular alterations can cause changes in cognitive performance (Novak and Hajjar, 2010). This interaction is made more complex by interindividual variation in cognitive reserve (Stern, 2012), which modulates the relationship between cognitive function and structural damage (magnetic resonance imaging, MRI) or impaired metabolism (positron emission tomography) (Fotenos et al., 2008; Garibotto et al., 2008). To shed light on the complex interplay between cognitive performance and neurovascular reserve, a better understanding of the link between cognitive deficits and brain pathology in the transition from healthy control subjects (HC) to amnestic mild cognitive impairment (aMCI) to AD could be provided by determining if alterations in cerebrovascular reserve, which can be assessed via a measurement of cerebrovascular reactivity (CVR), are linked to alterations in cognition.

The application of carbon dioxide (CO_2) induces vasodilation, which can be assessed in the entire brain parenchyma using blood oxygen level–dependent (BOLD) MRI (Cohen et al., 2002; Haller et al., 2006, 2008; Kassner and Roberts, 2004; Mutch et al., 2012; Ziyeh et al., 2005). Beyond changes in CVR amplitude, 1 previous functional magnetic resonance imaging (fMRI) study (Cantin et al., 2011) observed that a different slope of response to hypercapnia was found in MCI and AD patients than in control subjects,

* Corresponding author at: Service neuro-diagnostique et neuro-interventionnel DISIM, Hôpitaux Universitaires de Genève, Rue Gabrielle Perret-Gentil 4, 1211 Genève 14, Switzerland. Tel.: +41 (0) 22 37 23311; fax: +41 (0) 22 37 27072.
E-mail address: sven.haller@hcuge.ch (S. Haller).

0197-4580/$ – see front matter © 2015 Elsevier Inc. All rights reserved.
http://dx.doi.org/10.1016/j.neurobiolaging.2014.07.020

suggesting that the temporal dynamics of CVR may differ. In that study, however, the spatial distribution of these changes in timing was not studied, and no relationship between cognition and velocity was established. Other studies suggest that changes in the amplitude of CVR in AD is widely distributed across the brain: impaired CVR in frontal, parietal, and temporal lobes has been found using CT (Oishi et al., 1999), and BOLD-MRI studies (Cantin et al., 2011; Yezhuvath et al., 2012) showing that large-scale vascular changes are occurring with the disease. Coherently, resting-state BOLD fMRI investigations also demonstrated large-scale functional network alterations in dementia (Greicius et al., 2004), suggesting that studying regional changes across the whole brain yields additional insights into the spatial localization of differences between patients and control subjects. An additional motivation for studying changes at the regional level is that, in healthy control subjects at least, CVR is very regionally specific (Rostrup et al., 2000).

The current investigation tested the hypothesis that aMCI and AD patients exhibit abnormal vascular CVR dynamics, and that these abnormalities are related to cognition. To this end, we assessed the velocity of the regional CVR during a CO_2 challenge in aMCI and AD compared with healthy control subjects.

2. Methods

2.1. Subjects

The local ethical committee approved this prospective study; all participants gave written informed consent before inclusion. From our memory clinic, 63 subjects were prospectively included, including 20 AD patients, 15 aMCI patients, and 28 HC from the Basel Study on the Elderly (Monsch and Kressig, 2010). Groups were relatively well balanced for sex and age (Table 1) showing no significant differences. AD patients had lower Mini Mental State Examination (MMSE) scores but generally were minimally impaired.

The subjects were examined according to standard diagnostic procedures (Monsch and Kressig, 2010), including brain MRI without contrast agents. The diagnosis criteria for AD were based on the NINCDS-ADRDA criteria (McKhann et al., 1984). The diagnosis criteria for aMCI were based on Winblad et al. (2004).

2.2. Magnetic resonance imaging

Imaging was performed on a 3T clinical whole-body MRI scanner (Verio, Siemens Medical Systems, Erlangen, Germany). Standard routine clinical imaging included a 3D T1w (1 mm^3 isotropic, $256 \times 256 \times 176$ matrix). Additional sequences (T1w, T2w, T2*, and FLAIR) were acquired and analyzed to exclude brain pathology such as ischemic stroke, subdural hematomas, or space-occupying lesions and determine white matter lesion severity (Fazekas et al., 1987), Table 1.

Table 1
Demographic information

	HC	aMCI	AD
Number of subjects	28	15	20
Number of women (percentage)[a]	18 (64)	9 (60)	10 (50)
Average age (y) ± SD[b]	73 ± 7	71 ± 10	76 ± 7
Mean MMSE score ± SD[c]	29 ± 1	28 ± 2	25 ± 3
Median Fazekas score (range)[d]	1 (0–3)	1 (0–3)	1 (0–3)

Continuous measures are compared between groups using a 1-way ANOVA. Dichotomous variables: χ^2 test. Ordinal measures: Kruskal-Wallis test.
Key: AD, Alzheimer's disease; aMCI, amnestic mild cognitive impairment; ANOVA, analysis of variance; HC, healthy controls; MMSE, Mini Mental State Examination; SD: standard deviation.
[a] No significant difference between groups ($\chi^2 = 1.0$, $p = 0.61$).
[b] No significant difference between groups ($F = 1.9$, $p = 0.16$).
[c] Significant difference between groups ($F = 31.9$, $p < 10^{-9}$), no difference between HC and aMCI.
[d] No significant difference between groups ($\chi^2 = 0.12$, $p = 0.94$).

The 9 minutes CO_2 challenge consisted of CO_2 administered via a nasal cannula in a concentration of 7% mixed in synthetic air, with the sequence 1 minute OFF, 2 minutes ON, 2 minutes OFF, 2 minutes ON, 2 minutes OFF (details in the following). Subjects were asked to breathe normally through the nose. Simultaneous multi-echo echo-planar imaging (EPI) covering the entire brain was acquired with the following parameters: 64×48 matrix, 34 slices, voxel size of $3.44 \times 3.44 \times 3.5$ mm^3, echo times of 12.3, 29.5, 46.8, and 64 ms, repetition time of 2970 ms, 180 repetitions.

We deliberately chose a very simple experimental setup, consisting of a gas bottle with a ready for use mix of 7% CO_2 and synthetic air. This gas bottle was outside the MRI in the control room and connected via a simple silicone tube to a standard nasal cannula in the MRI room. The technician manually started and stopped the CO_2 application at 8 L/min using a standard clinical flow meter. Note that much more sophisticated setups exist including automatic synchronization with the MRI sequence and use of tight face masks to segregate inflow and outflow with the ability to measure expiratory CO_2 concentration. Such a setup is in our experience the most appropriate for a research setting in younger individuals, as for example tight face masks are oftentimes not well tolerated by elderly individuals.

2.3. Preprocessing

Data were preprocessed using SPM8 (version 5236, http://fil.ion.ucl.ac.uk/spm/). For BOLD analysis, the second echo of the EPI sequence was used. Functional images were motion corrected (realignment to the mean image). The T1w structural image was segmented and normalized ("new segment" algorithm). Functional images were coregistered to the normalized T1w structural image. The structural images were parcellated into 90 cortical and subcortical gray matter regions using the AAL atlas (Tzourio-Mazoyer et al., 2002). The bilateral globus pallidus was removed from the data because of characteristic segmentation issues related to its small size in the atlas, leaving 88 regions. EPI data were averaged within each atlas region, yielding 88 regionally averaged time series per subject with improved signal-to-noise ratio compared with individual voxelwise data. Each time series was rescaled by the grand mean computed over all atlas regions of the corresponding subject and linearly detrended. The 6 translation and rotation parameters from the realignment procedure were regressed out. Finally, each time course was Winsorized to the 5th and 95th percentile to minimize the effect of any remaining intensity spikes.

For voxel-based morphometry (VBM) analysis, the VBM8 toolbox (http://dbm.neuro.uni-jena.de/vbm/) was used. T1w images were normalized to MNI space (DARTEL warping, default ICBM template). The resulting normalized gray matter segments were modulated to account for spatial normalization. The data were smoothed by convolution with an 8 mm-FWHM Gaussian kernel.

2.4. Statistical analyses

Analyses were performed using Matlab R2012b and the statistics and optimization toolboxes version R2012b (Mathworks, Natick, MA, USA), as well as R 3.0.2 with the stats 3.0.2, nlme 3.1-113, car 2.0-19, multcomp 1.3-1, and effects 2.3 packages (R Foundation for Statistical Computing, Vienna, Austria).

2.4.1. VBM analysis

For visual quality assurance of the homogeneity of the data, the sample covariance matrix was displayed, as well as 1 slice per

image. A group-level full factorial GLM was created by entering the normalized, modulated individual gray matter volumes as predictors, and a categorical ternary group membership variable (HC, MCI, or AD) as a covariate. The model parameters were estimated, and pairwise contrasts (HC > MCI, HC > AD, and MCI > AD) were computed. Multiple comparison correction was applied using familywise error rate (FWER).

2.4.2. CVR analysis

Studies of hypercapnia typically use end-tidal CO_2 time courses measured in vivo as a regressor for the BOLD signal (Cantin et al., 2011). In our setup, no end-tidal CO_2 levels are monitored, and the regressors are therefore defined analytically. A CO_2 challenge regressor was defined by convolving the CO_2 on-off timing vector with a filter whose frequency response is given as:

$$H(\omega) = \frac{c}{1 + (1 - c)e^{-\omega}}$$

where c is a constant, leading to an exponential washin and washout behavior (see Fig. 1). c was set to 0.15, to obtain a shape similar to previous work (Jiang et al., 2010; Rieger et al., 2012; Stefanovic et al., 2006) (see Fig. 3 e.g., fits). Note that in Jiang et al. (2010) a similar regressor was obtained by convolving the CO_2 timing vector with a gamma function, also exhibiting the exponential behavior. We denote that the "nominal" CO_2 regressor, meaning that it represents the expected response in healthy subjects, based on the literature. A second CO_2 regressor with $c = 0.11$ was computed, representing a slower vessel dilation and lower slope during the steady-state phase of hypercapnia (Cantin et al., 2011). This was denoted as the "slow" CO_2 regressor. Linear combinations of these regressors give rise to a flexible family of possible BOLD response time courses, representing the various possible dynamics of the CVR. Regressors were shifted by 1 repetition time (3 seconds) to account for hemodynamic lag. The 2 regressors were normalized to unit peak-to-peak amplitude, demeaned, and orthogonalized (Fig. 1). The principle of using linear combinations of regressors to obtain a more flexible temporal representation is similar to adding temporal derivative to the canonical hemodynamic response function (Friston et al., 1998), except that in our case the effect of adding the "slow" regressor is to modify slopes of the washin and washout, instead of shifting the basis functions forward or backward (note also that the "slow" regressor is not the derivative of the "nominal" regressor).

Two CO_2 regression coefficients (denoted β_1, β_2) were estimated per region (88 per subject) using constrained least squares fitting (Matlab function lsqlin), imposing positivity of the β_1 coefficient to ensure physiological plausibility of the linear combination of regressors. A negative β_2 value corresponds to a slower response than

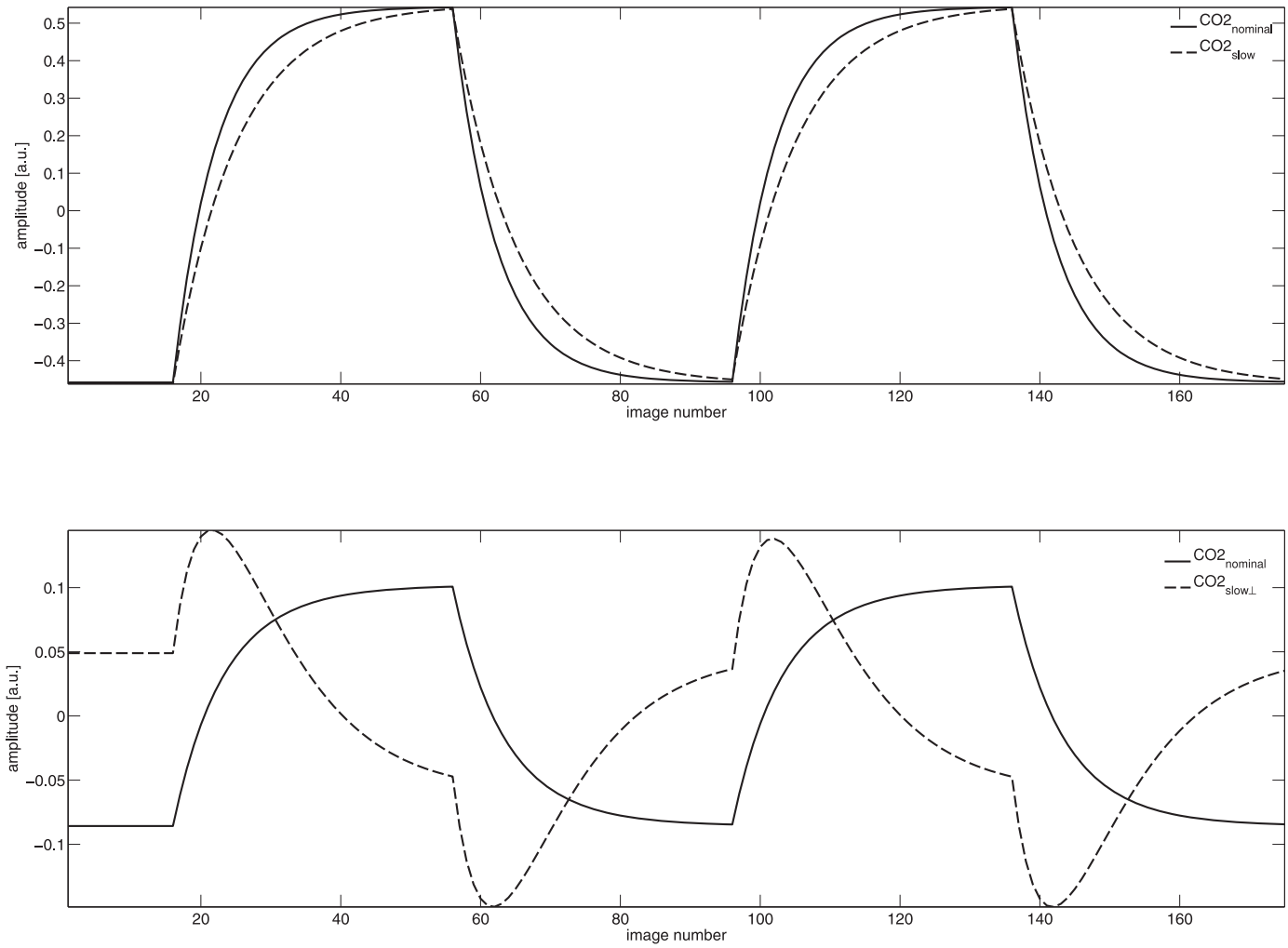

Fig. 1. Model regressors for CO_2 challenge. Time courses of the "nominal" (continuous line) and "slow" (dashed line) CO_2 challenge regressors. The top panel shows the regressors before orthogonalization, whereas the bottom panel shows them as entered in the design matrix.

modeled by the nominal regressor, whereas a positive β_2 value corresponds to a faster response. Thus, β_2 models CVR velocity (representing the rate of vasodilation or vasoconstriction, and controlling the initial slope of the washin and washout periods), whereas β_1 models amplitude. Showing a correspondence with the sigmoid conceptual model relating blood flow change to partial pressure of CO_2 (Sobczyk et al., 2014), a Gompertz sigmoid function can be fit to our linear combination of regressors with very high goodness of fit (R^2 around 0.99), and the β_2 parameter has a clear influence on the Gompertz growth rate parameter. Each region was subsequently represented by its β_1 or β_2 CVR coefficient value in second-level analyses. Model fit was assessed by an F-test.

Four main analyses were performed: (1) overall effect; (2) lobe level; (3) regional level; and finally; (4) relationship between CVR parameters and cognitive scores. For the overall analysis, a 3-way mixed-effects ANOVA with diagnostic group and lobe as main effects, subject as random effect, and subject nested in group was conducted on the β_1 and β_2 values, via a linear mixed model. Comparisons on group effect were performed using the Benjamini-Hochberg step-down procedure (FDR) to adjust the reported p-value for multiple comparisons (Benjamini and Hochberg, 1995). In lobe-level analysis, to yield insights into the spatial location of differences and enable comparison with the literature (Cantin et al., 2011), brain regions were grouped into 7 lobes (Tzourio-Mazoyer et al., 2002), and the data for each lobe were modeled using a separate linear mixed-effect model, with group as main effect, subject as random effect, and subject nested in group. Tukey contrasts (HC > aMCI, HC > AD, and aMCI > AD) were computed for the main effect of group in each model. Within each pairwise contrast, the uncorrected p-values were compared with a significance threshold FDR-adjusted for the number of lobes. For the region-level analysis, pairwise contrasts were computed between diagnostic groups for all 88 regions, using a 1-sided 2-sample t test assuming unequal variance, and results were FDR corrected. In addition, a receiver operating characteristic analysis was performed for each region, using 1000 bootstrap replicates to compute a confidence interval on the area under curve. The relationship between CVR coefficients and any residual motion was tested by a linear mixed model regressing the CVR velocity or amplitude coefficient on 12 summary motion parameters (average and maximum x, y, z translations, and pitch, roll, and yaw rotations for each subject), with subject as random effect, and subject nested in group. The relationship between CVR coefficients and global gray matter atrophy was tested by a linear mixed model regressing the CVR velocity or amplitude coefficient on gray matter volume (obtained from VBM analysis), with subject as random effect, and subject nested in group. We also tested the relationship between CVR coefficients and microangiopathy by performing the same analysis as for gray matter volume, but with Fazekas scores.

Finally, the relationship between CVR coefficients and cognitive scores was modeled at the regional level by the full cognitive model $\beta_2 = 1 + \text{gender} + \text{age} + \text{MMSE} + \text{age:MMSE}$. A baseline model $\beta_2 = 1 + \text{gender} + \text{age}$ was also used for comparison. Model fit was assessed by F-test. Effect plots were computed (R effects package).

3. Results

3.1. Structural voxelwise analysis

No subjects were excluded after quality assurance. VBM analysis showed no significant difference between HC and aMCI groups ($\alpha = 0.05$, FWER corrected) in gray matter density. The AD group showed a few locations with significant gray matter reductions ($p < 0.05$ FWER, peak T-value 8.62) including the hippocampal formation, as well as in the right medial temporal gyrus, right superior temporal gyrus, and left uncus and left amygdala. Also compared with aMCI, the AD group had significant gray matter density reductions ($p < 0.05$ FWER, peak T-value 6.28), located in the left parahippocampal area and with smaller spatial extent. There were no differences between HC and aMCI in gray matter density. As shown below (region-level analysis), areas of reduced gray matter density in VBM do not correspond to regions that have a trend for differences in CVR velocity.

3.2. CVR analysis

3.2.1. Overall analysis

Subjects reported no discomfort during MR imaging and CO_2 administration.

There was a significant main effect of group ($\chi^2 = 6.09$, $p = 0.048$) and lobe ($\chi^2 = 85.76$, $p < 10^{-15}$) on CVR velocity. There was no significant effect of group on CVR amplitude ($\chi^2 = 1.02$, $p = 0.600$) but a significant effect of lobe ($\chi^2 = 817.68$, $p < 10^{-15}$). CVR velocity was significantly larger in control subjects than in aMCI ($z = 1.03$, $p = 0.034$ FDR) and AD patients ($z = 0.99$, $p = 0.034$ FDR). Control subjects (HC) had a positive group mean CVR velocity (mean and standard error: 0.77 ± 0.03), whereas patients had a negative group mean CVR velocity (aMCI: -0.26 ± 0.06, AD: -0.22 ± 0.06), indicating that CVR in control subjects was on average faster than the nominal response, whereas CVR in patients was slower than nominal. These values correspond to a mean time to reach 90% of peak response of 33 seconds for HC and 59 seconds for aMCI and AD. There was no significant difference in CVR velocity between aMCI and AD.

There was no significant relationship between gray matter volume and CVR velocity ($\chi^2 = 1.42$, $p = 0.234$) nor between Fazekas score (representing microangiopathy severity) and CVR velocity ($\chi^2 = 0.23$, $p = 0.633$). There was also no significant relationship between CVR velocity and any of the 12 motion parameters ($\chi^2 = 0.07–1.51$, $p = 0.786–0.219$ uncorrected).

3.2.2. Lobe-level analysis

In the HC > aMCI contrast on CVR velocities, no lobe passed the FDR-corrected significance threshold, although values were low. The most different lobe was the occipital lobe ($t = 2.21$, $p = 0.014$ uncorrected), whereas the least different was the central lobe ($t = 1.36$, $p = 0.087$ uncorrected). For the HC > AD contrast, all lobes except central and the subcortical pseudo-lobe (putamen, caudate, and thalamus) had significantly higher velocities in control subjects than in patients ($p = 0.028$ FDR). No significant difference in velocity between aMCI and AD was found in the aMCI > AD contrast. No contrast showed a significant difference in CVR amplitude. Fig. 2 (A) shows the distribution of CVR velocity values for all groups and lobes. Fig. 2 (B) shows the brain space map of the effect size of CVR velocity in the HC > AD contrast in lobes. Supplementary Table 1 shows the statistics for the 3 contrasts on CVR velocity.

3.2.3. Region-level analysis

There were no significant pairwise differences in either the HC > aMCI or HC > AD contrasts on CVR velocity in regions after FDR correction for multiple comparisons. Four regions had a trend for differences in the HC > aMCI contrast ($p < 0.01$ uncorrected) in superior left occipital gyrus, left cuneus, and orbital part of the inferior frontal gyrus. Four regions had a trend for differences in the HC > AD contrast ($p < 0.01$ uncorrected) in bilateral straight gyri, right posterior cingulate, and left precuneus. Supporting the hypothesis of regional differences between groups, uncorrected p-values were generally low (HC > aMCI: median, 0.051 and range, 0.002–0.272; HC > AD: median, 0.048 and range, 0.004–0.441. The full distribution is shown in Supplementary Table 2 and

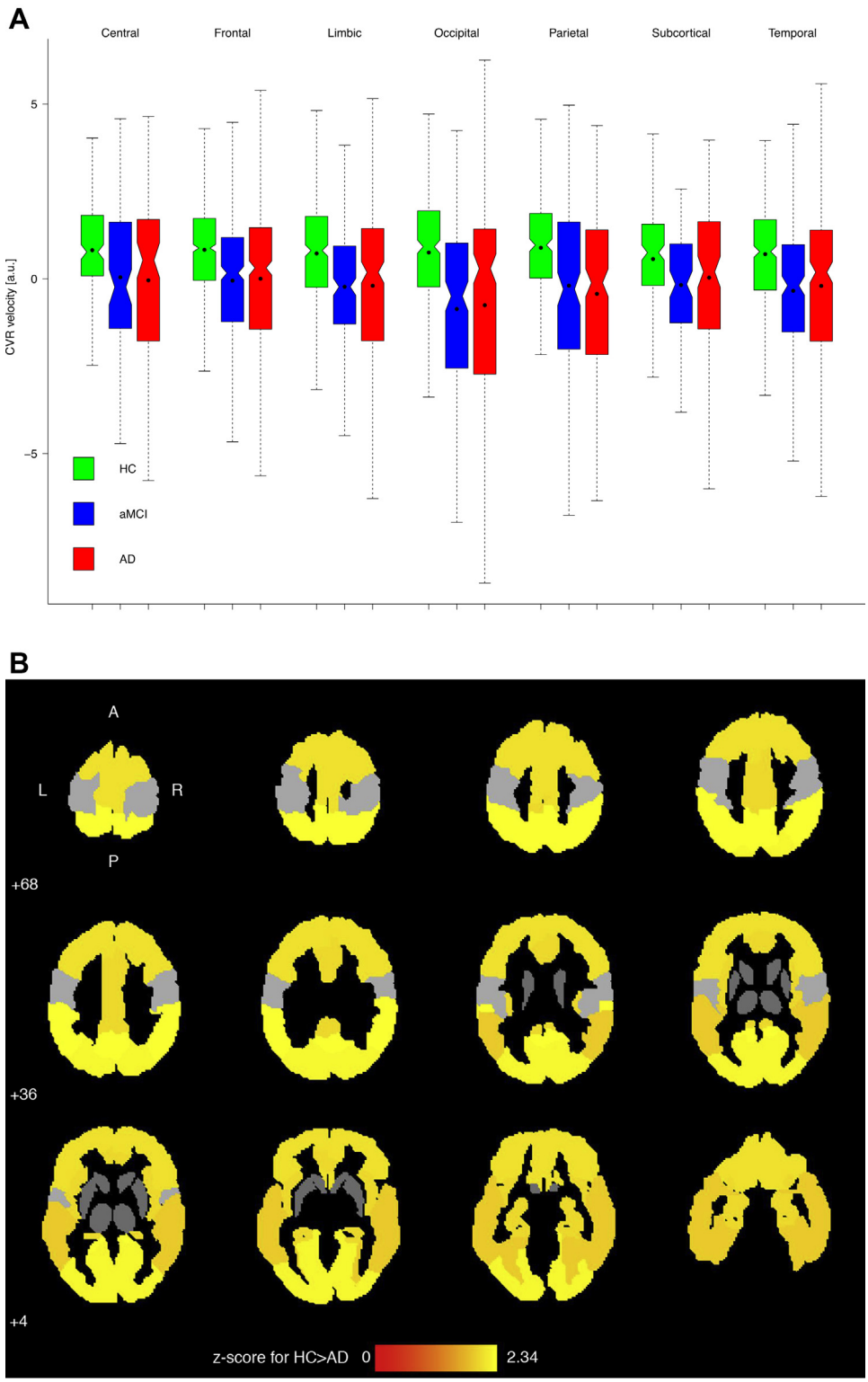

Fig. 2. Lobe-level differences in CVR velocity. (A) Distribution of CVR velocity parameter values for HC (green), aMCI (blue), and AD (red) groups in each lobe. The notch indicates the median, whereas the black dot indicates the mean of the distribution of values, and outliers are not shown. Patients have lower velocities than control subjects, but there is no difference between aMCI patients and AD patients. (B) Axial view of differences in CVR velocity at the lobe level, in neurologic convention. Lobes are colorized by equivalent z-score for the *p*-value of the lobe-wise contrast HC > AD for the difference in CVR velocity. The brightest color (yellow) corresponds to a z-score of 2.34, whereas the darkest color (red) maps to 0. All lobes except the central and the subcortical pseudo-lobe (shown in gray) show significant difference between groups ($p = 0.028$ FDR). The occipital and frontal lobes show the largest difference in CVR velocity. Abbreviations: AD, Alzheimer's disease; aMCI, amnestic mild cognitive impairment; CVR, cerebrovascular reactivity; FDR, false discovery rate; HC, healthy controls. (For interpretation of the references to color in this figure, the reader is referred to the web version of this article.)

Supplementary Fig. 1). The median area under curve value of the control subjects versus patients (aMCI + AD) receiver operating characteristic analysis of CVR velocity in the 88 regions was 0.64 (range, 0.55–0.72; confidence interval lower bound above 0.5 in 35 regions), indicating that the CVR velocity parameter has some limited diagnostic power, to a various degree depending on the region. Note these regions do not exhibit significant differences between groups in gray matter density, as shown by the VBM analysis. No significant difference was found in the aMCI > AD contrast, and uncorrected *p*-values were generally high (median, 0.524 and range, 0.092–0.857). Regional time courses for the HC > aMCI and HC > AD contrasts are illustrated in Fig. 3.

3.2.4. Relationship between CVR and cognitive scores

Thirty-five regions had a significant model fit ($p = 0.019$ FDR; minimum adjusted R^2, 0.12; maximum, 0.25; mean and SD, 0.17 ± 0.03, corresponding on average to a large effect size) and showed a significant positive relationship between MMSE and CVR ($p = 0.037$ FDR), as well as a significant negative age × MMSE interaction ($p = 0.038$ FDR). Ten regions of the DMN showed a significant fit: the left anterior and posterior cingulates, bilateral precuneus, bilateral middle frontal gyri, left parietal inferior gyrus, bilateral angular gyri, and left middle temporal gyrus (the mapping between default-mode network and the corresponding 26 AAL labels is found in Fransson and Marrelec, 2008; Richiardi et al., 2012). In the temporal lobe, only 1 of 14 regions was significant, instead of the expected 6 regions if the proportion of significant regions was equal across all lobes. The baseline model with only age and gender had no significant fits, suggesting that MMSE and age × MMSE interaction are indeed related to CVR velocity. Supplementary Table 2 shows coefficients of determination and corresponding F-test *p*-value for all regional models. Fig. 4 shows the brain space map of the equivalent z value for the *p*-values of the region-level F-test for model fit of CVR velocity on MMSE, age, and their interaction, corrected by gender.

In the regions with a significant fit, MMSE had a positive relationship with CVR velocity, and this relationship was modulated by age. The interaction between age and MMSE was antagonistic, that is, the relationship between MMSE and CVR velocity is smaller when age is higher. Fig. 5 shows the moderating effect of age on the relationship between MMSE interaction plot for subjects who are at the mean age in our sample (73), as well as 1 standard deviation above (81) and below (65). Microangiopathy severity was not a significant predictor (over 88 regions; t-statistic range, −0.835 to 2.284; median, 0.461; uncorrected *p*-value range, 0.026–0.988; median, 0.629).

4. Discussion

Using a simple and well-tolerated MR imaging paradigm, we found that the neurocognitive decline in aMCI and AD, as represented by MMSE score, is paralleled by reduced CVR velocity, and that this change in velocity is not related to general or focal gray matter atrophy, microangiopathy, or motion.

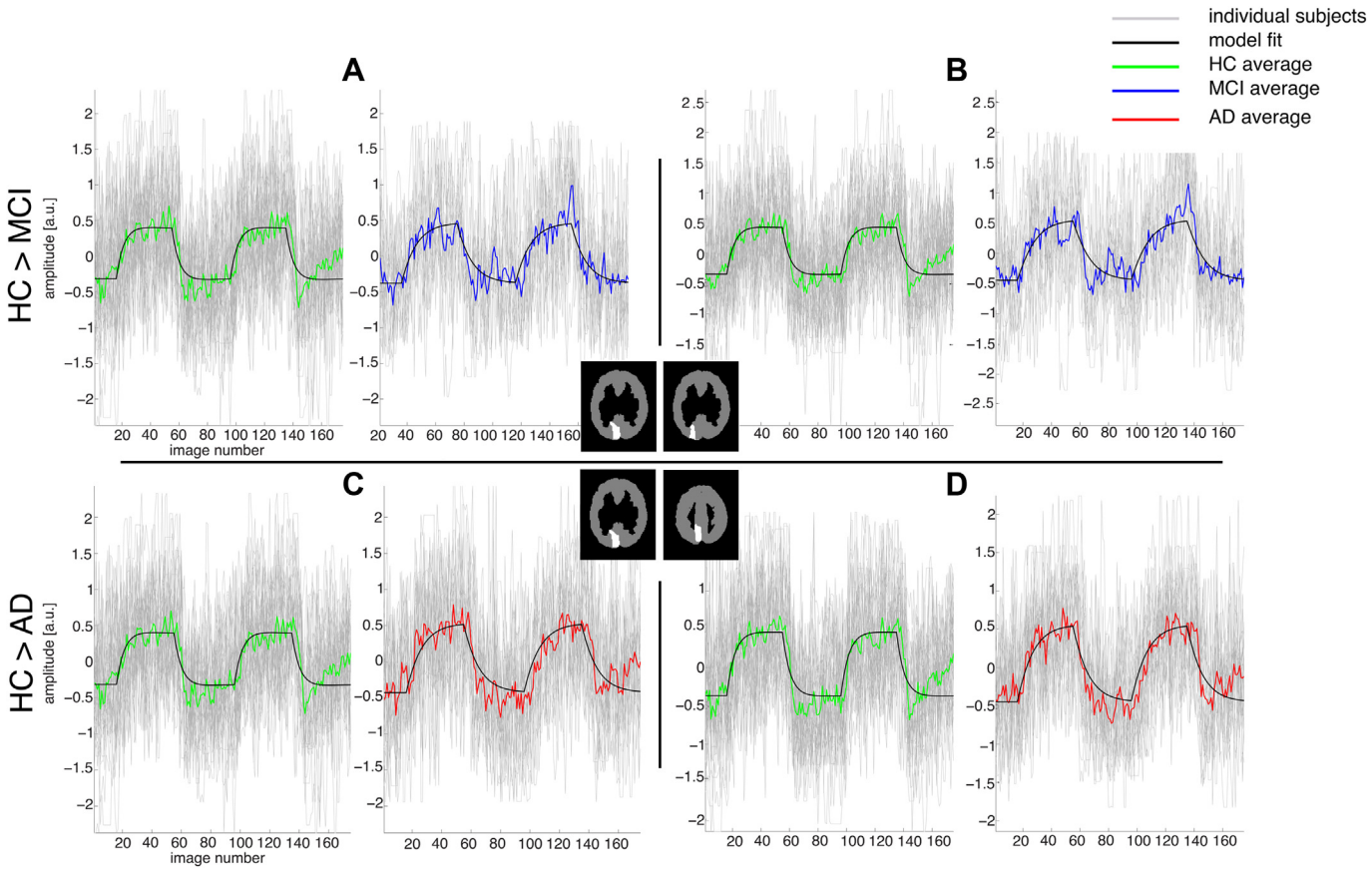

Fig. 3. Illustrative regional time courses in control subjects and patients. Regional time courses for all subjects (gray lines) and their average (green for HC, blue for aMCI, and red for AD), and model predicted response (black). Illustrative regions with the most difference in CVR velocity parameter and significant average model fit across subjects in both groups. Top row: HC > aMCI, bottom row: HC > AD. (A) Left cuneus ($p = 0.007$ uncorrected), (B) left superior occipital gyrus ($p = 0.002$ uncorrected), (C) left cuneus ($p = 0.01$ uncorrected), (D) left precuneus ($p = 0.007$, uncorrected). The insets show an axial view through the mean z-coordinate of the corresponding region, highlighted in white. Patients' response is noticeably slower than control subjects' in reaching steady state. Abbreviations: AD, Alzheimer's disease; aMCI, amnestic mild cognitive impairment; CVR, cerebrovascular reactivity; HC, healthy controls. (For interpretation of the references to color in this figure, the reader is referred to the web version of this article.)

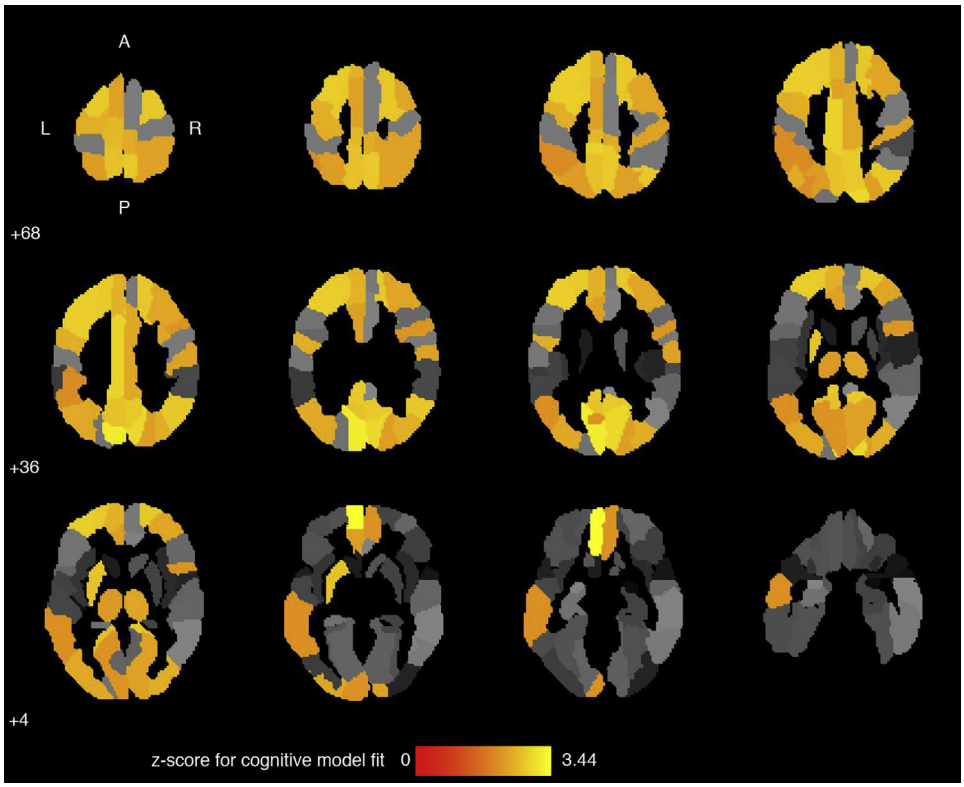

Fig. 4. Relationship between CVR velocity and MMSE score. Axial view of the relationship between CVR velocity parameter and MMSE score at the regional level, in neurologic convention. Regions are colorized by equivalent z-score for the *p*-value of the full cognitive model fit (comprising age, gender, MMSE, and age × MMSE). The brightest color (yellow) corresponds to a z-score of 3.44, whereas the darkest color (red) maps to 0. Regions with insignificant relationship between MMSE and CVR velocity are shown in gray, whereas regions with an orange-yellow hue show a significant association ($p = 0.019$ FDR). Note, that this relationship is particularly strong in frontal and occipital areas, whereas temporal areas show less effect. Abbreviations: CVR, cerebrovascular reactivity; MMSE, Mini Mental State Examination. (For interpretation of the references to color in this figure, the reader is referred to the web version of this article.)

4.1. CVR velocity in AD

Decreased CVR velocity is consistent with literature. In a visual task fMRI experiment, AD patients were shown to have widespread decreases of early response, corresponding to delayed response to a stimulus (Rombouts et al., 2005). Velocity decreases have also been observed in mouse models of AD, with slower return to the normal diameter of blood vessels after a vasoconstrictive drug was applied (Rancillac et al., 2012). Although many neurovascular factors may contribute to the difference between control subjects and patients in CVR velocity, changes in vessel stiffness would be consistent with our observations. Sabayan et al. (2012) reported in a meta-analysis that AD patients have higher pulsatility index (Gosling and King, 1974) in the middle cerebral artery, indicating higher downstream resistance. Results on pulse wave velocity also suggest stiffer vessels in AD, which may contribute to our observed velocity differences. Ten regions of the DMN had a significant association between MMSE and CVR velocity. This is noteworthy because reductions and desynchronization of the DMN are consistently reported in resting-state fMRI studies of MCI and AD without CO_2 challenge (Barkhof et al., 2014; Greicius et al., 2004). Such a decrease in functional connectivity can be explained by a number of factors, one of which may be regional differences in CVR velocity (itself potentially modulated by spontaneous respiration rate changes during resting state; Murphy et al., 2013).

4.2. CVR velocity and cognitive performance

The frontal and occipital lobes are notable because they have significantly lower CVR velocity in patients, and several regions where lower CVR velocity is associated with lower MMSE scores, a widely used and accepted yet coarse measure of the overall cognitive status. This agrees with previous studies reporting abnormal CVR in the frontal lobe of patients (Cantin et al., 2011; Yezhuvath et al., 2012). Because the amplitude of cerebral blood flow in the frontal lobe is not significantly different between control subjects and patients under CO_2 challenge (Cantin et al., 2011; Oishi et al., 1999), this velocity difference could be functionally relevant in cognitive performance. This is consistent with reports of a positive correlation between CVR amplitude and MMSE score in several lobes (Cantin et al., 2011) and between CVR amplitude and Boston Naming Test scores in the frontal lobe (Yezhuvath et al., 2012) (although that study found no correlation with MMSE). Alternatively, a difference of baseline function could also explain the CVR velocity difference between groups. For example, MCI can lead to higher neuronal activation when performing simple cognitive tasks (Kochan et al., 2010). Thus, although the aMCI subjects in our study can maintain relatively intact cognitive function (MMSE slightly but not significantly lower than control subjects), their vascular reserve is already showing signs of depletion, as reflected in our results. Conversely, it has been reported that AD and MCI patients have a widespread decrease in baseline T2* signal (Rombouts et al., 2007), although it was ascribed to gray matter atrophy differences which are mostly insignificant in our data. The dynamics difference observed in our results, where cognitive demands are minimal, could stem from a possible nonlinearity of vessel dilation speeds: vessel dilation in patients could start from a different baseline (either higher or lower) than control subjects. Finally, the modulatory effect of age on the relationship between MMSE and CVR velocity can be attributed to several factors, for example, increasing medication or hypertension with age could disrupt the relationship. Additionally, age-related cholinergic system impairment could

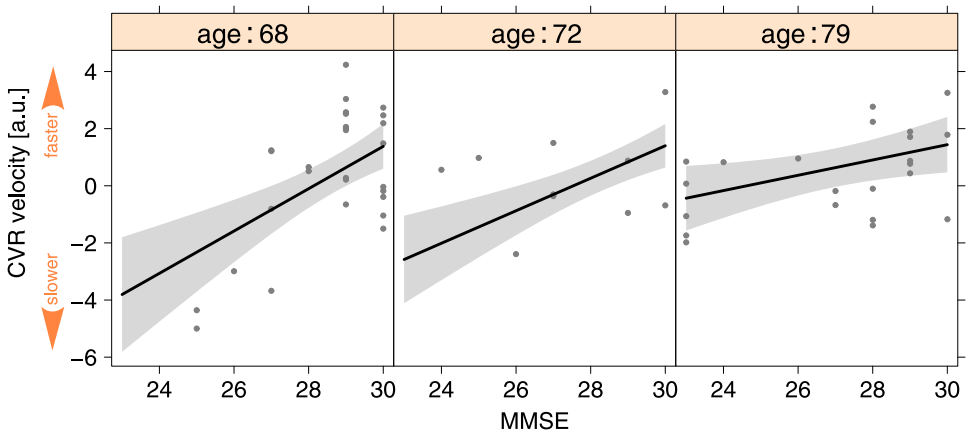

Fig. 5. Age modulates the relationship between CVR velocity and cognitive performance. The relationship between cognitive performance and CVR velocity is modulated by age. This plot, for the left cuneus, shows that a higher CVR velocity (higher value) corresponds to a higher MMSE score for relatively younger subjects. Subjects in the lowest and highest 5% of MMSE scores were trimmed for display (leaving 60 cases). The left panel shows the relationship if a subject is 68 years old (first quartile of the trimmed sample), whereas the middle and right panel show the relationship if a subject is 72 years old (median) and 79 year old, respectively (third quartile). The gray band shows the 95% confidence interval for the regression line. The dots indicate partial residuals (conditional on the age in that panel). Abbreviations: CVR, cerebrovascular reactivity; MMSE, Mini Mental State Examination. (For interpretation of the references to color in this figure, the reader is referred to the web version of this article.)

impact both CVR function and cognitive performance (Glodzik et al., 2013).

In the absence of established reference methods for in vivo assessment of cognitive reserve in the workup of cognitive decline, this study offers an additional vascular parameter, CVR velocity, which is linked to cognition and could be used in future studies as a factor to model when examining the cognitive reserve hypothesis, in addition to more established measures such as blood flow or structural and/or volumetric features.

4.3. CVR dynamics assessment in clinical practice

The clinical protocol used is easy to administer and well-tolerated by patients with aMCI and mild AD. The simple on-off "square wave" CO_2 stimulus is straightforward to apply and a robust probe for CVR dynamics (Mutch et al., 2012). Our results show that a simple nasal cannula is sufficient to induce significant whole-brain BOLD response under CO_2 challenge with acceptable acquisition time, and the setup necessary for the CO_2 clinical protocol does not interfere with the structural MRI typically performed in routine workup on cognitive decline. The alternative setup including a tight facemask segregating inflow and outflow allows not only more accurate application of CO_2 but also assessing expiratory CO_2 concentrations and is clearly more accurate in a research setting. However, there are constraints for the clinical applications, which should be considered. The experimental setup should be simple, inexpensive, and easy to use; attributes of the nasal cannula setup of the current investigation yet not of setups with tight facemasks requiring additionally devices to apply and measure CO_2 as well as compensation of the airflow resistance induced by the facemask. Moreover, a tight facemask setup substantially reduces patient comfort and in our experience further increased already present head motion artifacts (Haller et al., 2014). Standard MR imaging is routinely performed for the workup of neurocognitive decline in many centers. In our opinion, one of the fundamental requirements for the CVR assessment in this setting is the minimal interference with this standard MR imaging. Using a tight facemask, there are 2 options. The first option is installing the facemask during the entire MR imaging, yet this unnecessary reduces the patient comfort even during anatomic imaging and probably increases motion artifacts. The other option is installing the facemask after structural imaging only before the CVR imaging. This however requires additional installation during MR imaging, potentially the need to repeat scout scans, thereby prolonging the total measurement time. In contrast, the nasal cannula is easily and rapidly installed, does not interfere with anatomic imaging, and was well tolerated by all participants. Our setup is very simple and cheap, takes less than a minute to put in place, was well tolerated by all participants, did not interfere with standard MRI imaging, and can with only minimal demands be applied in any MRI center and clinical routine. The only requirement is the gas bottle with a ready to use mix of CO_2, whereas silicone tubes and nasal canals are standard equipments in most centers.

4.4. Limitations of the study

There were several limitations to this study. First, the relatively low number of aMCI patients and lack of follow-up could explain not finding a difference with AD patients. Although our results show that CVR dynamics are also impaired in aMCI patients, it is possible that changes in aMCI converters are gradual and could not be observed here. Second, our model cannot distinguish between dilation (washin) and contraction (washout) velocities because a single parameter controls both, but it is possible that they are differentially affected by disease status and progression. Third, our results do not show a difference in the CVR velocity of the hippocampus or parahippocampal formation. This may be because of field inhomogeneity in that region, but literature on hippocampal blood flow differences in dementia is inconclusive; observed differences may depend on image processing choices (Binnewijzend et al., 2013). Fourth, the absence of differences in the amplitude of CVR between study groups might be related to the relatively weaker hypercapnic stimuli using a nasal cannula as compared with a tight facemask. As discussed previously, simple experimental setup and noninterference with routine structural MR imaging were fundamental prerequisites for our study setup. Consequently, we deliberately took into account the less potent application of CO_2. Fifth, proximal vascular stenosis could potentially confound the dynamics of the CVR assessment (Haller et al., 2008). This potential confound could in principle be assessed by adding MR angiography of the cerebral vessels. Finally, our measure of cognitive performance, MMSE, encompasses several functional domains: many functional aspects of cognition are affected by cognitive decline, and it would be interesting to pinpoint more specifically which cognitive domain links with CVR parameters.

4.5. Conclusion

In summary, aMCI and AD patients showed slower CVR response than control subjects to CO_2 BOLD challenge, and CVR response velocity was related to cognitive performance, modulated by age. The dynamics of cerebrovascular reactivity could be a useful tool in the study of the relationship between neurovascular reserve, cognitive performance, and cognitive reserve. CVR dynamics can be assessed by a simple and well-tolerated clinical protocol, enabling use of the technique in a routine clinical setting.

Disclosure statement

The authors have no actual or potential conflicts of interest.

Acknowledgements

This study was supported in part by a grant of the VELUX foundation, in part by a European Union Marie Curie International Fellowship (grant #299500), the Swiss National Science Foundation (grant PP00P2-146318), and the Novartis foundation. The authors thank the anonymous reviewers for their useful comments.

Appendix A. Supplementary data

Supplementary data associated with this article can be found, in the online version, at http://dx.doi.org/10.1016/j.neurobiolaging.2014.07.020.

References

Barkhof, F., Haller, S., Rombouts, S.A., 2014. Resting-state functional MR imaging: a new Window to the brain. Radiology 272, 29–49.
Benjamini, Y., Hochberg, Y., 1995. Controlling the false discovery rate: a practical and powerful approach to multiple testing. J. R. Statisl. Soc. B 57, 289–300.
Binnewijzend, M.A., Kuijer, J.P., Benedictus, M.R., van der Flier, W.M., Wink, A.M., Wattjes, M.P., van Berckel, B.N., Scheltens, P., Barkhof, F., 2013. Cerebral blood flow measured with 3D pseudocontinuous arterial spin-labeling MR imaging in Alzheimer disease and mild cognitive impairment: a marker for disease severity. Radiology 267, 221–230.
Cantin, S., Villien, M., Moreaud, O., Tropres, I., Keignart, S., Chipon, E., Le Bas, J.F., Warnking, J., Krainik, A., 2011. Impaired cerebral vasoreactivity to CO2 in Alzheimer's disease using BOLD fMRI. Neuroimage 58, 579–587.
Claassen, J.A., Diaz-Arrastia, R., Martin-Cook, K., Levine, B.D., Zhang, R., 2009. Altered cerebral hemodynamics in early Alzheimer disease: a pilot study using transcranial Doppler. J. Alzheimers Dis. 17, 621–629.
Cohen, E.R., Ugurbil, K., Kim, S.G., 2002. Effect of basal conditions on the magnitude and dynamics of the blood oxygenation level-dependent fMRI response. J. Cereb. Blood Flow Metab. 22, 1042–1053.
Fazekas, F., Chawluk, J.B., Alavi, A., Hurtig, H.I., Zimmerman, R.A., 1987. MR signal abnormalities at 1.5 T in Alzheimer's dementia and normal aging. AJR Am. J. Roentgenol. 149, 351–356.
Fotenos, A.F., Mintun, M.A., Snyder, A.Z., Morris, J.C., Buckner, R.L., 2008. Brain volume decline in aging: evidence for a relation between socioeconomic status, preclinical Alzheimer disease, and reserve. Arch. Neurol. 65, 113–120.
Fransson, P., Marrelec, G., 2008. The precuneus/posterior cingulate cortex plays a pivotal role in the default mode network: evidence from a partial correlation network analysis. Neuroimage 42, 1178–1184.
Friston, K.J., Josephs, O., Rees, G., Turner, R., 1998. Nonlinear event-related responses in fMRI. Magn. Reson. Med. 39, 41–52.
Garibotto, V., Borroni, B., Kalbe, E., Herholz, K., Salmon, E., Holtoff, V., Sorbi, S., Cappa, S.F., Padovani, A., Fazio, F., Perani, D., 2008. Education and occupation as proxies for reserve in aMCI converters and AD: FDG-PET evidence. Neurology 71, 1342–1349.
Glodzik, L., Randall, C., Rusinek, H., de Leon, M.J., 2013. Cerebrovascular reactivity to carbon dioxide in Alzheimer's disease. J. Alzheimers Dis. 35, 427–440.
Gosling, R.G., King, D.H., 1974. Arterial assessment by Doppler-shift ultrasound. Proc. R. Soc. Med. 67, 447–449.
Greicius, M.D., Srivastava, G., Reiss, A.L., Menon, V., 2004. Default-mode network activity distinguishes Alzheimer's disease from healthy aging: evidence from functional MRI. Proc. Natl. Acad. Sci. U.S.A 101, 4637–4642.
Haller, S., Bonati, L.H., Rick, J., Klarhofer, M., Speck, O., Lyrer, P.A., Bilecen, D., Engelter, S.T., Wetzel, S.G., 2008. Reduced cerebrovascular reserve at CO2 BOLD MR imaging is associated with increased risk of periinterventional ischemic lesions during carotid endarterectomy or stent placement: preliminary results. Radiology 249, 251–258.
Haller, S., Monsch, A.U., Richiardi, J., Barkhof, F., Kressig, R.W., Radue, E.W., 2014. Head motion parameters in fMRI differ between patients with mild cognitive impairment and Alzheimer disease versus elderly control subjects. Brain Topogr. http://www.ncbi.nlm.nih.gov/pubmed/24599620?dopt=Citation [Epub ahead of print].
Haller, S., Wetzel, S.G., Radue, E.W., Bilecen, D., 2006. Mapping continuous neuronal activation without an ON-OFF paradigm: initial results of BOLD ceiling fMRI. Eur. J. Neurosci. 24, 2672–2678.
Jiang, Z., Krainik, A., David, O., Salon, C., Tropres, I., Hoffmann, D., Pannetier, N., Barbier, E.L., Bombin, E.R., Warnking, J., Pasteris, C., Chabardes, S., Berger, F., Grand, S., Segebarth, C., Gay, E., Le Bas, J.F., 2010. Impaired fMRI activation in patients with primary brain tumors. Neuroimage 52, 538–548.
Kassner, A., Roberts, T.P., 2004. Beyond perfusion: cerebral vascular reactivity and assessment of microvascular permeability. Top Magn. Reson. Imaging 15, 58–65.
Kochan, N.A., Breakspear, M., Slavin, M.J., Valenzuela, M., McCraw, S., Brodaty, H., Sachdev, P.S., 2010. Functional alterations in brain activation and deactivation in mild cognitive impairment in response to a graded working memory challenge. Dement Geriatr. Cogn. Disord. 30, 553–568.
McKhann, G., Drachman, D., Folstein, M., Katzman, R., Price, D., Stadlan, E.M., 1984. Clinical diagnosis of Alzheimer's disease: report of the NINCDS-ADRDA Work Group under the auspices of Department of Health and Human Services Task Force on Alzheimer's Disease. Neurology 34, 939–944.
Monsch, A.U., Kressig, R.W., 2010. Specific care program for the older adults: memory clinics. Eur. Geriatr. Med. 1, 128–131.
Murphy, K., Birn, R.M., Bandettini, P.A., 2013. Resting-state fMRI confounds and cleanup. Neuroimage 80, 349–359.
Mutch, W.A., Mandell, D.M., Fisher, J.A., Mikulis, D.J., Crawley, A.P., Pucci, O., Duffin, J., 2012. Approaches to brain stress testing: BOLD magnetic resonance imaging with computer-controlled delivery of carbon dioxide. PLoS One 7, e47443.
Novak, V., Hajjar, I., 2010. The relationship between blood pressure and cognitive function. Nat. Rev. Cardiol. 7, 686–698.
Oishi, M., Mochizuki, Y., Takasu, T., 1999. Regional differences in cerebrovascular reactivity to acetazolamide in Alzheimer's disease. J. Clin. Neurosci. 6, 380–381.
Rancillac, A., Geoffroy, H., Rossier, J., 2012. Impaired neurovascular coupling in the APPxPS1 mouse model of Alzheimer's disease. Curr. Alzheimer Res. 9, 1221–1230.
Richiardi, J., Gschwind, M., Simioni, S., Annoni, J.M., Greco, B., Hagmann, P., Schluep, M., Vuilleumier, P., Van De Ville, D., 2012. Classifying minimally disabled multiple sclerosis patients from resting state functional connectivity. Neuroimage 62, 2021–2033.
Rieger, S.W., Pichon, S.P.V., 2012. Sensitivity mapping and comparison of T2*-weighted conventional and multiplexed MRI sequences using a hypercapnic challenge. European Society for Magnetic Resonance in Medicine and Biology Annual Meeting.
Rombouts, S.A., Goekoop, R., Stam, C.J., Barkhof, F., Scheltens, P., 2005. Delayed rather than decreased BOLD response as a marker for early Alzheimer's disease. Neuroimage 26, 1078–1085.
Rombouts, S.A., Scheltens, P., Kuijer, J.P., Barkhof, F., 2007. Whole brain analysis of T2* weighted baseline FMRI signal in dementia. Hum. Brain Mapp. 28, 1313–1317.
Rostrup, E., Law, I., Blinkenberg, M., Larsson, H.B., Born, A.P., Holm, S., Paulson, O.B., 2000. Regional differences in the CBF and BOLD responses to hypercapnia: a combined PET and fMRI study. Neuroimage 11, 87–97.
Sabayan, B., Jansen, S., Oleksik, A.M., van Osch, M.J., van Buchem, M.A., van Vliet, P., de Craen, A.J., Westendorp, R.G., 2012. Cerebrovascular hemodynamics in Alzheimer's disease and vascular dementia: a meta-analysis of transcranial Doppler studies. Ageing Res. Rev. 11, 271–277.
Sobczyk, O., Battisti-Charbonney, A., Fierstra, J., Mandell, D.M., Poublanc, J., Crawley, A.P., Mikulis, D.J., Duffin, J., Fisher, J.A., 2014. A conceptual model for CO2-induced redistribution of cerebral blood flow with experimental confirmation using BOLD MRI. Neuroimage 92, 56–68.
Stefanovic, B., Warnking, J.M., Rylander, K.M., Pike, G.B., 2006. The effect of global cerebral vasodilation on focal activation hemodynamics. Neuroimage 30, 726–734.
Stern, Y., 2012. Cognitive reserve in ageing and Alzheimer's disease. Lancet Neurol. 11, 1006–1012.
Tzourio-Mazoyer, N., Landeau, B., Papathanassiou, D., Crivello, F., Etard, O., Delcroix, N., Mazoyer, B., Joliot, M., 2002. Automated anatomical labeling of activations in SPM using a macroscopic anatomical parcellation of the MNI MRI single-subject brain. Neuroimage 15, 273–289.
Winblad, B., Palmer, K., Kivipelto, M., Jelic, V., Fratiglioni, L., Wahlund, L.O., Nordberg, A., Backman, L., Albert, M., Almkvist, O., Arai, H., Basun, H., Blennow, K., de Leon, M., DeCarli, C., Erkinjuntti, T., Giacobini, E., Graff, C., Hardy, J., Jack, C., Jorm, A., Ritchie, K., van Duijn, C., Visser, P., Petersen, R.C., 2004. Mild cognitive impairment–beyond controversies, towards a consensus: report of the International Working Group on Mild Cognitive Impairment. J. Intern. Med. 256, 240–246.
Yezhuvath, U.S., Uh, J., Cheng, Y., Martin-Cook, K., Weiner, M., Diaz-Arrastia, R., van Osch, M., Lu, H., 2012. Forebrain-dominant deficit in cerebrovascular reactivity in Alzheimer's disease. Neurobiol. Aging 33, 75–82.
Ziyeh, S., Rick, J., Reinhard, M., Hetzel, A., Mader, I., Speck, O., 2005. Blood oxygen level-dependent MRI of cerebral CO2 reactivity in severe carotid stenosis and occlusion. Stroke 36, 751–756.